arXiv:1401.0678v1 [physics.flu-dyn] 3 Jan 2014

Velocity-Gradient Probability Distribution Functions in a Lagrangian Model of Turbulence

L. Moriconi[1], R.M. Pereira[2] and L.S. Grigorio[3],

[1]*Instituto de Física, Universidade Federal do Rio de Janeiro,*

C.P. 68528, CEP: 21945-970, Rio de Janeiro, RJ, Brazil

[2]*Divisão de Metrologia em Dinâmica de Fluidos,*

Instituto Nacional de Metrologia, Normalização e Qualidade Industrial,

Av. Nossa Senhora das Graças 50, Duque de Caxias,

25250-020, Rio de Janeiro, Brazil and

[3]*Centro Federal de Educação Tecnológica Celso*

Suckow da Fonseca, 28635-000, Nova Friburgo, Brazil

Abstract

The Recent Fluid Deformation Closure (RFDC) model of lagrangian turbulence is recast in path-integral language within the framework of the Martin-Siggia-Rose functional formalism. In order to derive analytical expressions for the velocity-gradient probability distribution functions (vgPDFs), we carry out noise renormalization in the low-frequency regime and find approximate extrema for the Martin-Siggia-Rose effective action. We verify, with the help of Monte Carlo simulations, that the vgPDFs so obtained yield a close description of the single-point statistical features implied by the original RFDC stochastic differential equations.

PACS numbers: 47.27.Gs, 47.27.eb, 47.27.ef

I. INTRODUCTION

It has been long known, since the seminal work of Batchelor and Townsend [1], that spatial derivatives of a turbulent velocity field do not behave as gaussian random variables. The current view on this still barely understood phenomenon is that the non-gaussian fluctuations of the velocity gradients – the hallmark of turbulent intermittency – are likely to be related to the existence of long-lived coherent structures and to deviations from the Kolmogorov "K41" scaling, both important ingredients in the contemporary phenomenology of turbulence [2, 3].

The main notorious difficulties with first-principle theories of intermittency stand on (i) the inadequacy of perturbative expansions to deal with the coupled dynamics of vorticity and the rate-of-strain tensor at high Reynolds numbers and (ii) the fact that the closed equations for the time evolution of the velocity gradient tensor are non-local in the space variables. Notwithstanding the strong coupling/non-local issues, it is actually possible to devise simplified fluid dynamical models that would capture relevant qualitative features of the intermittent fluctuations of the velocity gradient tensor [4]. Here, a fundamental role is played by the lagrangian framework of fluid dynamics, since it leads in a natural way to reduced-dimensional systems, in the form of either ordinary or stochastic differential equations for the time evolution of the velocity gradient tensor [5–8].

The aforementioned lagrangian models have been mostly investigated by means of numerical integrations of the associated differential equations, which can then be compared to well-established results of alternative direct numerical simulations. There is, however, a large room for the exploration of analytical tools in the study of lagrangian models of intermittency, a direction we pursue here, joining other authors in this effort [7, 9]. We focus our attention on one particularly interesting stochastic model, the Recent Fluid Deformation Closure (RFDC) model [8], and derive reasonable approximations for its velocity gradient probability distribution functions (vgPDFs). We put into practice standard statistical field-theoretical procedures for the computation of effective actions through vertex renormalization [10, 11], which are carried out in the context of the Martin-Siggia-Rose functional formalism [12–15]. Our approach – essentially a semiclassical treatment – is general enough, so that, in principle, it can be applied to a large class of stochastic models.

This paper is organized as follows. In Sec. II, we briefly outline, as a ground for the subsequent discussions, the essential points of the RFDC model. In Sec. III, we rephrase

the RFDC model in the Martin-Siggia-Rose path-integral formalism and study it through the effective action method. Analytical expressions for the vgPDFs are then obtained. In Sec. IV, we compare, using Monte-Carlo simulations, our vgPDFs with the ones derived from the numerical integration of the RFDC differential stochastic equations. Finally, in Sec. V, we summarize our main findings and point out directions of further research.

II. THE RFDC LAGRANGIAN STOCHASTIC MODEL

Our central object of interest is the time-dependent lagrangian velocity gradient tensor $\mathbb{A}(t)$, which has cartesian components $A_{ij} = \partial_i v_j$. Taking, as a starting point, the Navier-Stokes equations with external gaussian stochastic forcing, the exact lagrangian evolution equation for $\mathbb{A}(t)$ is

$$\dot{\mathbb{A}} = V[\mathbb{A}] + g\mathbb{F} \ , \tag{1}$$

where $V[\mathbb{A}]$ is a functional of $\mathbb{A}$, defined as

$$V_{ij}[\mathbb{A}] = -(\mathbb{A}^2)_{ij} + \partial_i\partial_j\nabla^{-2}\mathrm{Tr}(\mathbb{A}^2) + \nu\nabla^2(\mathbb{A})_{ij} \ , \tag{2}$$

and $\mathbb{F}$ is a zero-mean, second order gaussian random tensor, which satisfies to

$$\langle F_{ij}(t)F_{kl}(t')\rangle = G_{ijkl}\delta(t-t') \ , \tag{3}$$

with

$$G_{ijkl} = 2\delta_{ik}\delta_{jl} - \frac{1}{2}\delta_{il}\delta_{jk} - \frac{1}{2}\delta_{ij}\delta_{kl} \ . \tag{4}$$

In Eq. (1), g is just an arbitrary coupling constant proportional to the external power per unit mass, which has an important role in our discussion, since it will be taken as an expansion parameter around the linearized model.

The second and third contributions to the right hand side of (2) are, respectively, the pressure Hessian (written as a non-local functional of the velocity gradient tensor) and the viscous dissipation term. As it stands, Eq. (2) is of course not closed: exact solutions on a single lagrangian trajectory are clearly dependent on the bulk space-time profiles of the velocity gradient tensor. However, motivated by the fact that $\mathbb{A}(t)$ is typically short-time correlated, it is natural to conjecture that both the pressure Hessian and the viscous dissipation term are dominated by local contributions. This is the point of view taken in the RFDC model of Chevillard and Meneveau [8], where these local contributions are related

to the Kolmogorov and the large eddy time scales of the flow, τ and T, respectively (the Reynolds number is, thus, $R_e \propto (T/\tau)^2$). It is then assumed that the lagrangian evolution of $\mathbb{A}(t)$ is associated, for small time scales, to the approximate Cauchy-Green tensor

$$\mathbb{C} = \exp[\tau\mathbb{A}]\exp[\tau\mathbb{A}^{\mathrm{T}}] \ , \tag{5}$$

so that the functional $V[\mathbb{A}]$ in Eq. (1) gets replaced by a local function of $\mathbb{A}$,

$$V(\mathbb{A}) = -\mathbb{A}^2 + \frac{\mathbb{C}^{-1}\mathrm{Tr}(\mathbb{A}^2)}{\mathrm{Tr}(\mathbb{C}^{-1})} - \frac{\mathrm{Tr}(\mathbb{C}^{-1})}{3T}\mathbb{A} \ . \tag{6}$$

We end up, therefore, with a closed and much simpler time evolution equation for $\mathbb{A}$:

$$\dot{\mathbb{A}} = V(\mathbb{A}) + g\mathbb{F} = -\mathbb{A}^2 + \frac{\mathbb{C}^{-1}\mathrm{Tr}(\mathbb{A}^2)}{\mathrm{Tr}(\mathbb{C}^{-1})} - \frac{\mathrm{Tr}(\mathbb{C}^{-1})}{3T}\mathbb{A} + g\mathbb{F} \ . \tag{7}$$

We refer the reader to Ref. [8] for a more detailed account on the conceptual and technical aspects of the RFDC model.

It is convenient to set $T = 1$ (without loss of generality) and perform an expansion of $V(\mathbb{A})$ up to some arbitrary power of τ in (6). A previous extensive numerical study shows that even the first order expansion is enough to grasp the physical content of the model [16]. We work, throughout the paper, with second order expansions of $V(\mathbb{A})$, which we write as

$$V(\mathbb{A}) = \sum_{p=1}^{4} V_p(\mathbb{A}) \ , \tag{8}$$

where

$$V_1(\mathbb{A}) = -\mathbb{A} \ , \tag{9}$$

$$V_2(\mathbb{A}) = -\mathbb{A}^2 + \frac{\mathbb{I}}{3}\mathrm{Tr}(\mathbb{A}^2) + \frac{2\tau}{3}\mathrm{Tr}(\mathbb{A})\mathbb{A} \ , \tag{10}$$

$$V_3(\mathbb{A}) = -\frac{\tau}{3}\left(\mathbb{A} + \mathbb{A}^{\mathrm{T}} - \frac{2\mathbb{I}}{3}\mathrm{Tr}(\mathbb{A})\right)\mathrm{Tr}(\mathbb{A}^2) - \frac{\tau^2}{3}\mathrm{Tr}(\mathbb{A}^{\mathrm{T}}\mathbb{A})\mathbb{A} - \frac{\tau^2}{3}\mathrm{Tr}(\mathbb{A}^2)\mathbb{A} \ , \tag{11}$$

$$V_4(\mathbb{A}) = -\frac{\mathbb{I}}{9}\tau^2\mathrm{Tr}(\mathbb{A}^{\mathrm{T}}\mathbb{A})\mathrm{Tr}(\mathbb{A}^2) - \frac{\mathbb{I}}{9}\tau^2[\mathrm{Tr}(\mathbb{A}^2)]^2 + \frac{\tau^2}{3}\mathbb{A}^{\mathrm{T}}\mathbb{A}\mathrm{Tr}(\mathbb{A}^2) + \\ + \frac{\tau^2}{6}(\mathbb{A}^2 + \mathbb{A}^{2\mathrm{T}})\mathrm{Tr}(\mathbb{A}^2) \ . \tag{12}$$

It is important to note that $V_p(\mathbb{A})$ comprises all the contributions of $O(\mathbb{A}^p)$ to $V(\mathbb{A})$. The RFDC model yields a promising stage for further improvements, insofar its vgPDFs as well as its geometrical statistical properties related to the coupling between the vorticity and the rate-of-strain tensor share several qualitative features in common with the ones observed in experiments and direct numerical simulations of turbulence [17, 18].

III. PATH-INTEGRAL FORMULATION OF THE RFDC MODEL

Assume that at time $t = 0$ the velocity gradient tensor is $\mathbb{A}(0) \equiv \mathbb{A}_0$. We may write, within the framework of the Martin-Siggia-Rose (MSR) functional formalism [12–15], the following path-integral expression for the conditional probability density function of finding, at time $t = \beta$, the velocity gradient tensor $\mathbb{A}(\beta) \equiv \mathbb{A}_1$,

$$\rho(\mathbb{A}_1|\mathbb{A}_0,\beta) \equiv \mathcal{N}\int_{\Sigma} D[\hat{\mathbb{A}}]D[\mathbb{A}]\exp\left\{-\int_0^{\beta} dt\left[i\mathrm{Tr}[\hat{\mathbb{A}}^{\mathrm{T}}L(\mathbb{A})] + \frac{g^2}{2}G_{ijkl}\hat{A}_{ij}\hat{A}_{kl}\right]\right\} , \qquad (13)$$

where

$$\Sigma = \{\mathbb{A}(0) = \mathbb{A}_0 \ , \ \mathbb{A}(\beta) = \mathbb{A}_1\} \qquad (14)$$

specifies the set of boundary conditions, $\mathcal{N}$ is a normalization factor, and

$$L(\mathbb{A}) \equiv \dot{\mathbb{A}} - V(\mathbb{A}) \ . \qquad (15)$$

In the above expression, $\hat{\mathbb{A}} = \hat{\mathbb{A}}(t)$ is just an auxiliary tensor field (a time-dependent 3×3 matrix) with no direct physical meaning. The conditional PDF given in Eq. (13) is nothing but a formal solution, written with path-integral dressing, of the Fokker-Planck equation that can be derived from the stochastic differential Eq. (7).

General Strategy for the derivation of vgPDFs

Taking $\beta \to \infty$ in the conditional PDF (13), we obtain the stationary vgPDF evaluated at $\mathbb{A}_1$, which is expected to be independent from the initial condition $\mathbb{A}_0$. Also, as it is clear from the original RFDC equations, in the limit of small g, nonlinear perturbations become negligible and all we get are gaussian distributions for the vgPDFs. We are, thus, interested to investigate how the vgPDFs evolve as the noise strength g gets progressively larger and intermittency effects cannot be neglected anymore. Straightforward semiclassical evaluations can be implemented, in principle, along two alternative procedures [10, 11]: (i) in the WKB approach, quadratic fluctuations around the classical Euler-Lagrange equations of motion are tentatively integrated; (ii) in the Effective Action method, the path-integral can be evaluated up to some order in perturbation theory and Euler-Lagrange equations are then subsequently studied.

In both methods (i) and (ii), it is necessary to deal with variational Euler-Lagrange equations which take into account the boundary conditions in Σ, as defined in (14). However, it

is important to note that while in (i) the integration over quadratic fluctuations boils down to the computation of a functional determinant, the perturbative expansion in (ii) is generally associated to the evaluation of one-loop Feynman diagrams. As it is well-known from standard field-theoretical arguments [11], the computation of the functional determinants in the WKB approach encodes, in general, a complet set of one-loop one-particle irreducible (1PI) Feynman diagrams, which turn out to be, in our case, of unfortunate cumbersome implementation. Within the Effective Action method, on the other hand, we can select the one-loop diagrams which we assume are the most relevant and check, *a posteriori*, how good will this selection perform. This is the pragmatic point of view that we follow throughout this work.

To start, we take profit of the independence of the conditional vgPDF (13) upon the initial condition $\mathbb{A}_0$, for $\beta \to \infty$, and impose the particular periodic boundary conditions

$$\mathbb{A}(0) = \mathbb{A}(\beta) = \bar{\mathbb{A}} \ . \tag{16}$$

As it will be clear a bit later, the choice of periodic boundary conditions for $\mathbb{A}(t)$ is very convenient, once it leads to great simplifications in the structure of the effective action. We may state, therefore, that up to an unimportant renormalization factor (which from now on is suppressed, for convenience, from all the PDF expressions),

$$\rho(\bar{\mathbb{A}}) \equiv \lim_{\beta\to\infty} \rho(\bar{\mathbb{A}}|\bar{\mathbb{A}}, \beta) = \exp\{-S_c[\hat{\mathbb{A}}^c, \mathbb{A}^c]\} \tag{17}$$

is the probability density function of having $\mathbb{A}(t) = \bar{\mathbb{A}}$ at an arbitrary time instant t in the asymptotic stationary fluctuation regime. In (17), $S_c[\hat{\mathbb{A}}^c, \mathbb{A}^c]$ is the "Effective Martin-Siggia-Rose Action", which satisfies to

$$\left.\frac{\delta S_c[\hat{\mathbb{A}}^c, \mathbb{A}]}{\delta A_{ij}}\right|_{\mathbb{A}=\mathbb{A}^c} = 0 \ , \tag{18}$$

$$\left.\frac{\delta S_c[\hat{\mathbb{A}}, \mathbb{A}^c]}{\delta \hat{A}_{ij}}\right|_{\hat{\mathbb{A}}=\hat{\mathbb{A}}^c} = 0 \ , \tag{19}$$

subject to the boundary conditions $\mathbb{A}^c(0) = \mathbb{A}^c(\beta) = \bar{\mathbb{A}}$. The index c used in Eqs. (17-19) stands for "classic", following the spread field-theoretical jargon.

If we are able to handle the Euler-Lagrange Eqs. (18) and (19) to write $\hat{\mathbb{A}}$ in terms of $\mathbb{A}$, then we may define

$$S_c[\mathbb{A}] \equiv S_c[\hat{\mathbb{A}}(\mathbb{A}), \mathbb{A}] \ . \tag{20}$$

We have, therefore,

$$\left.\frac{\delta S_c[\mathbb{A}]}{\delta A_{ij}}\right|_{\mathbb{A}^c} = \left.\frac{\delta S_c[\hat{\mathbb{A}}^c,\mathbb{A}]}{\delta A_{ij}}\right|_{\mathbb{A}=\mathbb{A}^c} + \left.\frac{\delta S_c[\hat{\mathbb{A}},\mathbb{A}^c]}{\delta \hat{A}_{kl}}\right|_{\hat{\mathbb{A}}=\hat{\mathbb{A}}^c} \times \left.\frac{\delta \hat{A}_{kl}}{\delta A_{ij}}\right|_{\mathbb{A}=\mathbb{A}^c} = 0 \ . \tag{21}$$

In other words, in order to find the vgPDF (17), it is necessary to solve just for one extrema $\mathbb{A}^c(t)$ of effective action $S_c[\mathbb{A}]$, as obtained from Eq. (21), instead of considering, in an explicit way, the solutions of both Eqs. (18) and (19).

The effective MSR action can be systematically evaluated to arbitrary degrees of precision. As a working hypothesis, we focus our attention only on the effects of noise renormalization, which amounts to say that the kernel $G_{ijkl}\delta(t-t')$, implicit in (13), gets substituted by a corrected one, $G^{ren}_{ijkl}(t-t')$, so that

$$S_c[\hat{\mathbb{A}},\mathbb{A}] = i\int_0^\beta dt \mathrm{Tr}[\hat{\mathbb{A}}^{\mathrm{T}} L(\mathbb{A})] + \frac{g^2}{2}\int_0^\beta dt \int_0^\beta dt' G^{ren}_{ijkl}(t-t')\hat{A}_{ij}(t)\hat{A}_{kl}(t') \ . \tag{22}$$

The saddle-point equations (18) and (19) give, respectively,

$$i\dot{\hat{A}}_{ij} + \hat{A}_{kl}\frac{\partial [V(\mathbb{A})]_{kl}}{\partial A_{ij}} = 0 \ , \tag{23}$$

$$iL_{ij}(\mathbb{A}) + g^2\int_0^\beta dt' G^{ren}_{ijkl}(t-t')\hat{A}_{kl}(t') = 0 \ . \tag{24}$$

It turns out that $G^{ren}_{iikl}(t-t') = G^{ren}_{ijkk}(t-t') = 0$ to all orders in perturbation theory, a result that is related to the fact that $\mathrm{Tr}(\mathbb{A}) = 0$ for the solutions of the RFDC equations. This leads, from Eq. (24), to $\mathrm{Tr}[L(\mathbb{A})] = 0$.

As it is usually done in effective action studies [10, 11], we work with low-frequency renormalization, once the saddle-point solutions are assumed to couple in a weak way to the fast degrees of freedom. We just mean here the replacement of the operator kernel $G^{ren}_{ijkl}(t-t')$ by $\tilde{G}^{ren}_{ijkl}\delta(t-t')$, where

$$\tilde{G}^{ren}_{ijkl} \equiv \int_{-\infty}^{\infty} dt G^{ren}_{ijkl}(t) \ . \tag{25}$$

Eq. (24) is transformed, in this way, into the local equation

$$iL_{ij}(\mathbb{A}) + g^2\tilde{G}^{ren}_{ijkl}\hat{A}_{kl} = 0 \ . \tag{26}$$

Taking into account now that $G^{ren}_{iikl} = G^{ren}_{ijkk} = 0$, we define,

$$\tilde{G}^{ren}_{ijkl} \equiv D_{ijkl} - \frac{1}{3}(x+y)\delta_{ij}\delta_{kl} \ , \tag{27}$$

where x and y are computable parameters, and

$$D_{ijkl} \equiv x\delta_{ik}\delta_{jl} + y\delta_{il}\delta_{jk} \ , \tag{28}$$

then Eq. (26) can be rewritten as

$$g^2 D_{ijkl}\hat{A}_{kl} = -iL_{ij}(\mathbb{A}) + \frac{g^2}{3}(x+y)\mathrm{Tr}[\hat{\mathbb{A}}]\delta_{ij} \ , \tag{29}$$

which leads to

$$\hat{A}_{ij} = -\frac{i}{g^2}D^{-1}_{ijkl}L_{kl}(\mathbb{A}) + \frac{1}{3}\mathrm{Tr}[\hat{\mathbb{A}}]\delta_{ij} \ , \tag{30}$$

a traceless tensor. Substituting Eq. (30) in the effective action (22), we get, in the low-frequency regime,

$$S_c[\mathbb{A}] = \frac{1}{2g^2}\int_0^\beta dt \left[D^{-1}_{ijkl}L_{ij}(\mathbb{A})L_{kl}(\mathbb{A})\right] \ . \tag{31}$$

Note that it is not difficult at all to obtain D^{-1}_{ijkl}. Defining

$$D^{-1}_{ijkl} \equiv a\delta_{ik}\delta_{jl} + b\delta_{il}\delta_{jk} \ , \tag{32}$$

the tensorial equation $D^{-1}_{ijpq}D_{pqkl} = \delta_{ik}\delta_{jl}$ implies, after some simple algebra, that

$$\begin{cases} ax + by = 1 \\ ay + bx = 0 \end{cases} \ , \tag{33}$$

and, consequently,

$$a = -\frac{x}{y^2 - x^2} \ , \ b = \frac{y}{y^2 - x^2} \ . \tag{34}$$

Our general strategy, is, thus, very clear: we have to determine, firstly, the values of x and y, as they are introduced in the definitions (27) and (28) for the renormalized noise kernel. In second place, we study the saddle point solutions of the effective action (31). Once we have these ingredients at hand, we can immediately write down an expression for the vgPDF in the RFDC model, viz,

$$\rho(\bar{\mathbb{A}}) = \exp\{-S_c[\mathbb{A}^c]\} \ , \tag{35}$$

where $S_c[\mathbb{A}^c]$ is given by Eq. (31), with $\mathbb{A}(t)$ substituted by $\mathbb{A}^c(t)$.

Noise Renormalization

The functional Taylor expansion of the effective action is obtained from the evaluation of operator kernels, which are identified to N-point 1PI Feynman diagrams [10, 11]. They

have, as a general rule, a prefactor that is proportional to the perturbative coupling constant (g^2 in our case) raised to a power which is directly related to the number of loops that each 1PI diagram contains.

The perturbative expansion is achieved very straightforwardly, in the path integral formulation, through the power series expansion of the exponentiated non-quadratic terms of the MSR action. The quadratic terms in the MSR action define the "free theory", where arbitrary expectation values, represented by the notation $\langle(...)\rangle_0$, can be exactly evaluated. In our particular problem, the free one-particle propagator is defined as

$$\langle A_{ij}(t)\hat{A}_{kl}(t')\rangle_0 = i\delta_{ik}\delta_{jl}G_0(t-t') \tag{36}$$

where

$$G_0(t-t') \equiv \Theta(t-t')\exp(t'-t) \tag{37}$$

is the Green's function of the differential operator

$$D_t \equiv 1 + \partial_t \ . \tag{38}$$

The renormalized noise kernel $G^{ren}_{ijkl}(t-t')$ is obtained from the relation

$$D_t D_{t'}\langle A_{ij}(t)A_{kl}(t')\rangle_{1PI} \equiv g^2 G^{ren}_{ijkl}(t-t') \ , \tag{39}$$

where $\langle(...)\rangle_{1PI}$ stands for the use of only 1PI contributions in the perturbative expansion of the expectation value under consideration. We have, up to $O(g^4)$,

$$D_t D_{t'}\langle A_{ij}(t)A_{kl}(t')\rangle_{1PI} = g^2[G_{ijkl}\delta(t-t') + g^2 C_{ijkl}(t-t')] \ , \tag{40}$$

where

$$C_{ijkl}(t-t') = \frac{1}{8}G_{abcd}G_{efgh}\int d\xi d\xi' \langle [V_2(\mathbb{A}(t))]_{ij}[V_2(\mathbb{A}(t'))]_{kl}\hat{A}_{ab}(\xi)\hat{A}_{cd}(\xi)\hat{A}_{ef}(\xi')\hat{A}_{gh}(\xi')\rangle_0 \ , \tag{41}$$

which means that $G^{ren}_{ijkl}(t-t') = G_{ijkl}\delta(t-t') + C_{ijkl}(t-t')$. The two contributions in the right-hand-side of (40) are represented by the two diagrams depicted in Fig. 1 [19]. The dashed lines in these diagrams are the external propagator lines which are removed in the 1PI contributions due to the action of the differential operators D_t and $D_{t'}$ in Eq. (39).

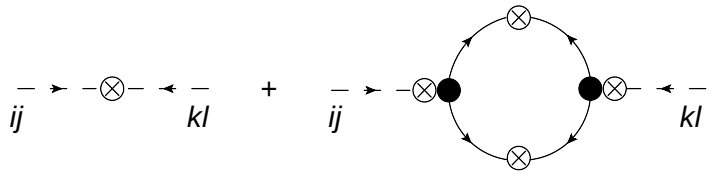

FIG. 1: The 1PI Feynman diagram contributions to the noise vertex renormalization of the effective Martin-Siggia-Rose action, up to $\mathrm{O}(g^4)$. The free one-particle propagators are represented by directed lines. The bare noise vertices are depicted as isolated crossed circles linked to two convergent lines. The bare three-point vertices are associated to the contributions provided by $V_2(\mathbb{A})$ in the RFDC stochastic time evolution equation (7).

Recalling the notation introduced in (27) and (28), we find, after straightforward computations,

$$x = 2 + \frac{3}{2}g^2 \ , \tag{42}$$

$$y = -\frac{1}{2} - \frac{1}{16}g^2 \ . \tag{43}$$

Taking into account, now, (32) and (34), the effective action (31) can be written, therefore, as

$$S_c[\mathbb{A}] = \frac{1}{2g^2}\int_0^\beta dt \left\{ a\mathrm{Tr}\left[L^{\mathrm{T}}(\mathbb{A})L(\mathbb{A})\right] + b\mathrm{Tr}\left[L^2(\mathbb{A})\right]\right\} \ . \tag{44}$$

Saddle-Point Solutions

It is a hard – if not an actually impossible – task to obtain the exact saddle-point solutions of the Euler-Lagrange equations (21) derived from the effective action (44). However, we can in principle retain, in the small g regime, only the quadratic terms in the effective action and use the saddle-point solutions obtained in this way as a first approximation to the exact solutions for larger values of g. We have, in the quadratic approximation,

$$S_c[\mathbb{A}] \equiv \frac{a}{2g^2}\int_0^\beta dt \mathrm{Tr}\left[\dot{\mathbb{A}}^{\mathrm{T}}\dot{\mathbb{A}} + \mathbb{A}^{\mathrm{T}}\mathbb{A}\right] + \frac{b}{2g^2}\int_0^\beta dt \mathrm{Tr}\left[\dot{\mathbb{A}}^2 + \mathbb{A}^2\right] \ . \tag{45}$$

The saddle-point Eq. (21) yields, in this case,

$$\ddot{\mathbb{A}} - \mathbb{A} = 0 \ . \tag{46}$$

The solution of (46) that satisfies the boundary conditions (14) is given by

$$\mathbb{A}(t) = \bar{\mathbb{A}} f_\beta(t) \ , \tag{47}$$

where

$$f_\beta(t) = 2\frac{\sinh(\frac{\beta}{2})}{\sinh(\beta)}\cosh(t - \frac{\beta}{2}) \ . \tag{48}$$

Substituting (47) in (8), we obtain

$$V(\mathbb{A}(t)) = \sum_{p=1}^{4} V_p(\bar{\mathbb{A}})[f_\beta(t)]^p \ . \tag{49}$$

The effective MSR action becomes, in the limit where $\beta \to \infty$,

$$S_c[\mathbb{A}^c] = S(\bar{\mathbb{A}}) = S_1(\bar{\mathbb{A}}) + S_2(\bar{\mathbb{A}}) \ , \tag{50}$$

with

$$S_1(\bar{\mathbb{A}}) = \frac{a}{2g^2}\mathrm{Tr}\left[I_1 \bar{\mathbb{A}}^{\mathrm{T}}\bar{\mathbb{A}} + \sum_{p=1}^{4}\sum_{q=1}^{4} I_{p+q} V_p(\bar{\mathbb{A}}^{\mathrm{T}}) V_q(\bar{\mathbb{A}})\right] \ , \tag{51}$$

and

$$S_2(\bar{\mathbb{A}}) = \frac{b}{2g^2}\mathrm{Tr}\left[I_1 \bar{\mathbb{A}}^2 + \sum_{p=1}^{4}\sum_{q=1}^{4} I_{p+q} V_p(\bar{\mathbb{A}}) V_q(\bar{\mathbb{A}})\right] \ , \tag{52}$$

where the above I-coefficients are defined as

$$I_1 = \lim_{\beta\to\infty}\int_0^\beta dt[\dot{f}_\beta(t)]^2 \ , \ I_{p+q} = \lim_{\beta\to\infty}\int_0^\beta dt[f_\beta(t)]^{p+q} \ . \tag{53}$$

Their numerical values are listed below

$$I_1 = I_2 = 1 \ , \ I_3 = 2/3 \ , \ I_4 = 1/2 \ , \ I_5 = 2/5 \ , \ I_6 = 1/3 \ , \ I_7 = 2/7 \ , \ I_8 = 1/4 \ . \tag{54}$$

We emphasize, at this point, that the number of terms that contribute to $S(\bar{\mathbb{A}})$ would be unnecessarily larger had we not used periodic boundary conditions for $\mathbb{A}^c(t)$. The reason is that due to the periodic boundary conditions, the several time integrations of tensorial products involving only one time derivative of the velocity gradient tensor can be removed from the effective action evaluated at its saddle-point configurations.

IV. ANALYTICAL VERSUS EMPIRICAL vgPDFs

Plots of the analytical vgPDFs $\rho(\bar{\mathbb{A}}) \propto \exp[-S(\bar{\mathbb{A}})]$ can be compared to the empirical PDFs obtained through the direct numerical solutions of the stochastic differential Eq. (7).

We have produced, using the analytical vgPDFs, large Monte Carlo ensembles of velocity gradients. The numerical solution of Eq. (7), on the other hand is carried out within a second order predictor-corrector method [20], with time step $\epsilon = 0.01$. We have considered, in all our numerical tests, $\tau = 0.1$, a reference time-scale usually taken in studies of the RFDC model.

In our Monte Carlo procedure, the velocity gradient $\mathbb{A}$ is additively perturbed by random traceless 3×3 matrices at each iteration step. The stochastic increments can be always written as a linear superposition of matrices of the overcomplete set $\{\mathbb{B}_1, \mathbb{B}_2, ..., \mathbb{B}_9\}$, where

$$\mathbb{B}_1 = \begin{bmatrix} 0 & 0 & 0 \\ 0 & 0 & 1 \\ 0 & -1 & 0 \end{bmatrix} , \; \mathbb{B}_4 = \begin{bmatrix} 0 & 1 & 0 \\ 1 & 0 & 0 \\ 0 & 0 & 0 \end{bmatrix} , \; \mathbb{B}_7 = \begin{bmatrix} 1 & 0 & 0 \\ 0 & -\frac{1}{2} & 0 \\ 0 & 0 & -\frac{1}{2} \end{bmatrix} ,$$

$$\mathbb{B}_2 = \begin{bmatrix} 0 & 0 & 1 \\ 0 & 0 & 0 \\ -1 & 0 & 0 \end{bmatrix} , \; \mathbb{B}_5 = \begin{bmatrix} 0 & 0 & 0 \\ 0 & 0 & 1 \\ 0 & 1 & 0 \end{bmatrix} , \; \mathbb{B}_8 = \begin{bmatrix} -\frac{1}{2} & 0 & 0 \\ 0 & 1 & 0 \\ 0 & 0 & -\frac{1}{2} \end{bmatrix} ,$$

$$\mathbb{B}_3 = \begin{bmatrix} 0 & 1 & 0 \\ -1 & 0 & 0 \\ 0 & 0 & 0 \end{bmatrix} , \; \mathbb{B}_6 = \begin{bmatrix} 0 & 0 & 1 \\ 0 & 0 & 0 \\ 1 & 0 & 0 \end{bmatrix} , \; \mathbb{B}_9 = \begin{bmatrix} -\frac{1}{2} & 0 & 0 \\ 0 & -\frac{1}{2} & 0 \\ 0 & 0 & 1 \end{bmatrix} . \tag{55}$$

Observe that the above matrices are special generators of three-dimensional rotations $(\mathbb{B}_1, \mathbb{B}_2, \mathbb{B}_3)$, reflections $(\mathbb{B}_4, \mathbb{B}_5, \mathbb{B}_6)$ and shearing transformations $(\mathbb{B}_7, \mathbb{B}_8, \mathbb{B}_9)$. In more precise terms, the ensemble of velocity gradients is produced from successive stochastic perturbations of $\mathbb{A}$ given as

$$\mathbb{A} \to \mathbb{A}' = \mathbb{A} + s\mathbb{B}_p \; . \tag{56}$$

Let $\Delta S(s) \equiv S(\mathbb{A}') - S(\mathbb{A})$ and χ be a gaussian random variable which is sorted at each Monte Carlo step, with zero mean and some standard deviation σ, to be defined below. In order to set s in (56), the Metropolis algorithm [21] is then applied as follows:

(i) If $\Delta S(\chi) < 0$, take $s = \chi$, otherwise define $p = \exp[-\Delta S(\chi)]$ and go to step (ii).

(ii) Take $s = \chi$ with probability p and $s = 0$ with probability $1 - p$.

As it is usually done in analogous Monte Carlo simulation contexts [22], the numerical value of the standard deviation parameter σ is adjusted so that the case $s = 0$ is verified in about 50% of the Monte Carlo steps.

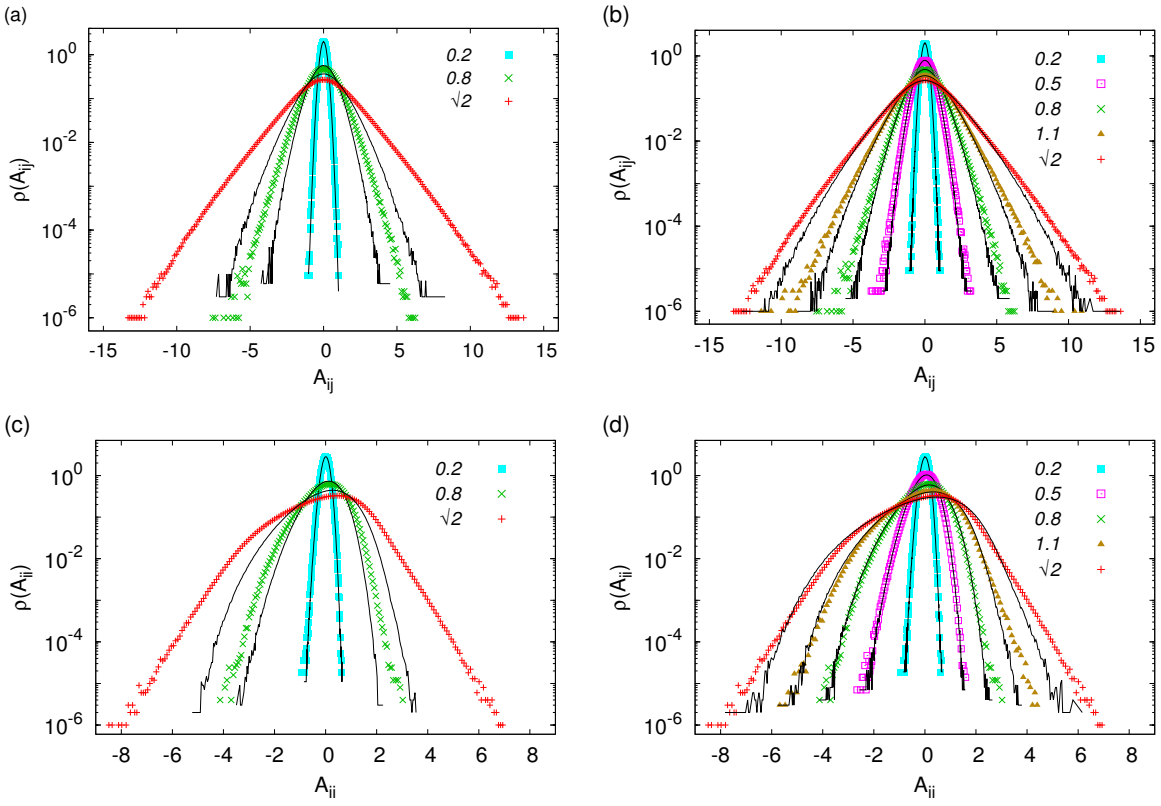

FIG. 2: Comparative semi-log plots of vgPDFs. The solid lines represent the analytical vgPDFs evaluated for $\tau = 0.1$ and some values of the bare noise strength g with and without noise renormalization. The vgPDFs depicted with symbols refer to the ones obtained from the direct numerical integration of the RFDC stochastic equations. The vgPDFs for the non-diagonal components of the velocity gradient tensor are given in figures (a) (nonrenormalized noise for g = 0.2, 0.8, and $\sqrt{2}$) and (b) (renormalized noise for g = 0.2, 0.5, 0.8, 1.1 and $\sqrt{2}$). The analogous results for the diagonal components are given in figures (c) and (d).

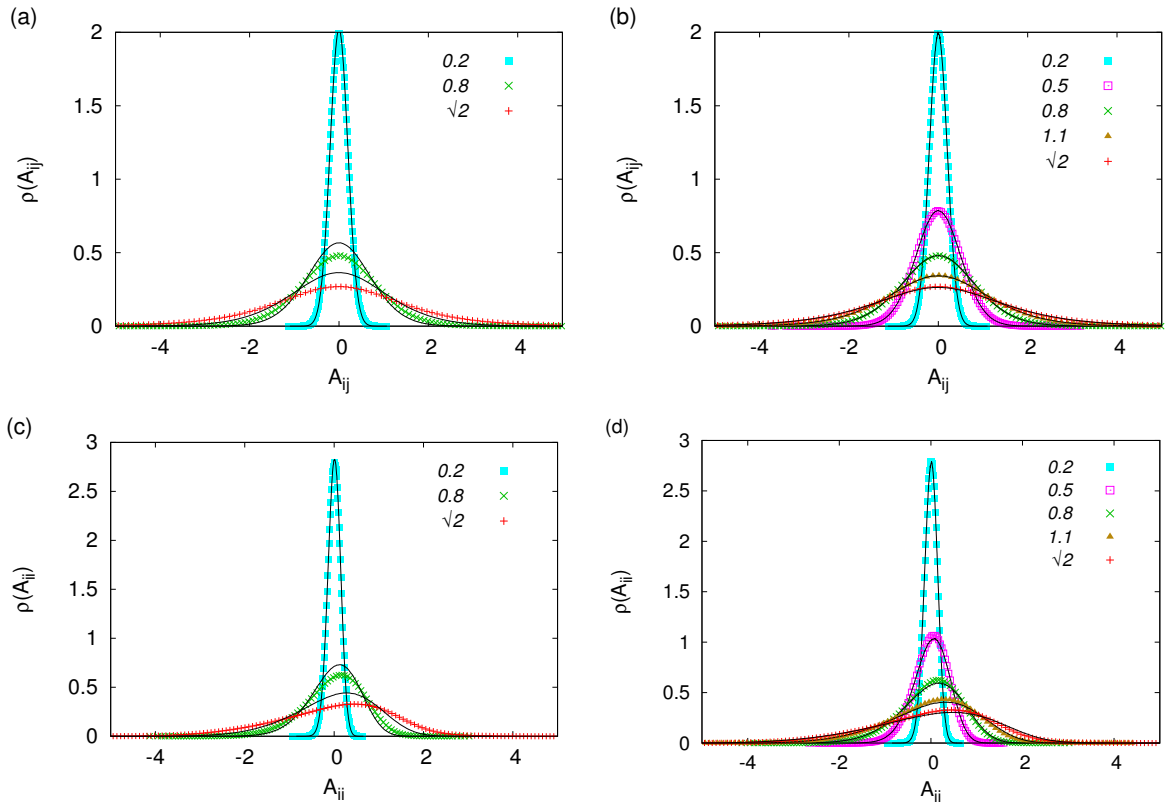

FIG. 3: Comparative linear plots of vgPDFs, described in the same way as in Fig. 2. The fittings in (b) and (d) are very reasonable within about two standard deviations around the peak values of the vgPDFs.

Samples of non-diagonal and diagonal components of the velocity gradient have been grouped into two distinct sets. We refer, thus, to vgPDfs of non-diagonal and diagonal components of $\mathbb{A}$, without specifying any particular cartesian tensor indices. Our statistical evaluations have been performed with sets of 12×10^6 and 24×10^6 elements for the diagonal and non-diagonal components, respectively, of the velocity gradient tensor.

Our results are shown in Figs. 2-4. In order to appreciate the relevance of noise renormalization, we also have depicted how would the vgPDFS look like if the noise vertex were not corrected by the loop diagram of Fig. 1 (these PDFs are given in Figs. 2a, 2c, 3a, and 3c). The one-loop correction leads, in fact, to much better approximations for the vgPDFs. The results are even more satisfactory to the eye if the vgPDFs are plotted in linear scales (Fig. 3), since larger deviations from the analytical expressions are found mostly in the far tails of the vgPDFs and are actually associated to small cumulative probabilities.

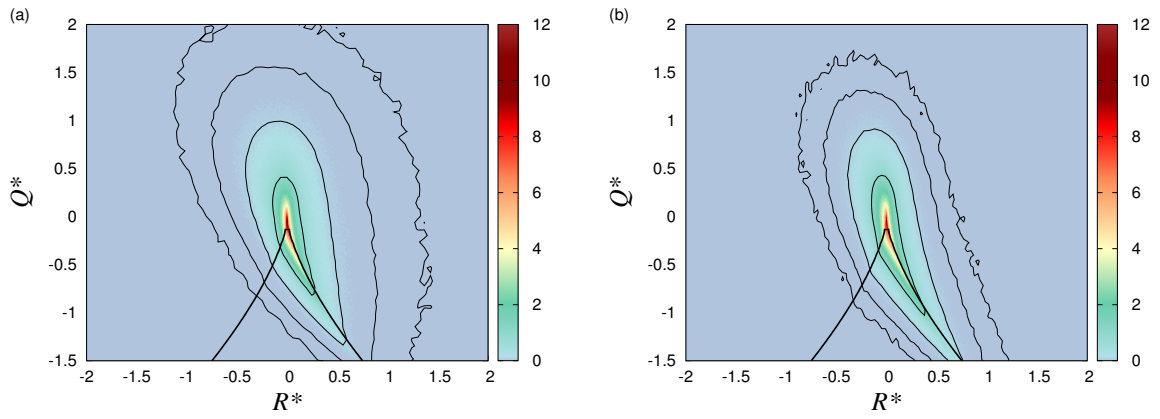

FIG. 4: Contour plots for the joint PDFs of the normalized Cayley-Hamilton invariants Q^* and R^* for $\tau = 0.1$ and $g = \sqrt{2}$. The level curves have PDF values equal to 1, 10^{-1}, 10^{-2} and 10^{-3}. Figure (a) is obtained from the the direct numerical integration of the RFDC stochastic equations, while figure (b) is evaluated from the analytical vgPDF discussed in Sec. III. The inverted V-shaped lines in both figures (a) and (b) indicate the Vieillefosse zero discriminant line.

In Fig. 4 we show how the analytical and the empirical joint probability distributions of the normalized Cayley-Hamilton invariants

$$Q^* = -\frac{\mathrm{Tr}(\mathbb{A}^2)}{2\langle S^2\rangle} \text{ and } R^* = -\frac{\mathrm{Tr}(\mathbb{A}^3)}{3\langle S^2\rangle^{3/2}} \,, \tag{57}$$

where S is the rate-of-strain tensor, with $S^2 \equiv S_{ij}S_{ij}$, compare to each other. We find that the analytical joint PDF is able to account for the essential qualitative geometrical features as the "tear-drop" shapes of the level curves and the role of the zero-discriminant line. The quantitative agreement is better, of course, close to the origin of the (R^*, Q^*) plane, where non-linear fluctuations of the velocity gradient tensor tend to be suppressed.

V. CONCLUSIONS

We have carried out an analytical study of the vgPDFs in the RFDC lagrangian model of turbulence. The MSR framework in its path-integral formulation proves to be a very convenient setup, where standard field-theoretical semiclassical approaches can be straightforwardly applied. Once it is difficult to establish exact saddle-point solutions for the Euler-Lagrange equations associated either to the bare or to the effective MSR action, we have used, as an approximation, solutions that hold in the regime of small noise strength. A

further source of technical difficulty is related to the precise evaluation of the effective MSR action up to one-loop order: in fact, one should take into account a large number of vertex corrections, leading to non-local kernels as the result of much more involved computations. We have, thus, put forward a pragmatical strategy for the evaluation of the effective MSR action where, as working hypotheses, (i) only the noise vertex is corrected up to one-loop order and (ii) a low-frequency approximation for the renormalized noise vertex is implemented. Nevertheless the above simplifying assumptions, the resulting analytical vgPDFs are satisfactorily compared to the empirical ones for a meaningful range of bare noise coupling constants ($g < \sqrt{2}$). We leave for additional research the necessary refinements on the approach we have adopted in this paper. We also note that time-dependent correlation functions of the velocity gradient tensor can be evaluated along similar semiclassical lines.

Analytical vgPDFs are a promising tool in the study of turbulent intermittency. Once validated, they can be used to investigate conditional statistics phenomena in a way that would be not possible through the ensembles produced from solutions of the related stochastic differential equations. A particularly interesting application of the analytical vgPDFS can be attempted, in principle, in the context of turbulent geometrical statistics, in order to clarify the statistical relations between the vorticity and the rate-of-strain fields.

It is important to emphasize, as a concluding remark, that the MSR semiclassical method as discussed in this work can be straightforwardly applied, with no further conceptual or technical obstacles, to several turbulence models and to a large class of phase-space reduced stochastic dynamical systems.

ACKNOWLEDEGMENTS

This work has been partially supported by CNPq and FAPERJ. The authors have greatly benefited from the use of NIDF facilities at COPPE-UFRJ. One of the authors (L.M.) would like to thank the warm hospitality of the ICTP during early stages of this work.

---

[1] G.K. Batchelor and A.A. Townsend, Proc. R. Soc. Lond. A **199**, 238 (1949).

[2] U. Frisch, *Turbulence: The Legacy of A.N. Kolmogorov*, Cambridge University Press (1995).

[3] P.A. Davidson, *Turbulence, an Introduction for Scientists and Engineers*, Oxford University

Press (2004).

[4] C. Meneveau, Ann. Rev. Fluid Mech. **43**, 219 (2011).

[5] P. Vieillefosse, Phys. A **125**, 150 (1984).

[6] B.J. Cantwell, Phys. Fluids A **4**, 782 (1992).

[7] M. Chertkov, A. Pumir and B.I. Shraiman, Phys. Fluids **11**, 2394 (1999).

[8] L. Chevillard and C. Meneveau, Phys. Rev. Lett. **97**, 174501 (2006).

[9] A. Naso, A. Pumir and M. Chertkov, J. Turb. **8**, 1 (2007).

[10] D. Amit, *Field Theory, Renormalization, and Critical Phenomena*, World Scientific Publishing Company (1984).

[11] J.J. Zinn-Justin, *Quantum Field Theory and Critical Phenomena*, Oxford University Press (2002).

[12] P.C. Martin, E.D. Siggia and H.A. Rose, Phys. Rev. A **8**, 423 (1973).

[13] H.K. Janssen, Z. Phys. **24**, 113 (1976).

[14] C. De Dominicis, J. Phys. C: Solid State Phys. **1**, 247 (1976).

[15] J. Cardy, *Scaling and Renormalization in Statistical Physics*, Cambridge University Press (1996).

[16] M.M. Afonso and C. Meneveau, Phys. D **239**, 1241 (2010).

[17] L. Chevillard and C. Meneveau, Phys. Fluids **23**, 101704 (2011).

[18] L. Chevillard, C. Meneveau, L. Biferale and F. Toschi, Phys. Fluids **20**, 101504 (2008).

[19] A well-written discussion on the perturbative diagrammatic expansions for stochastic differential equations can be found in A.-L. Barabasi and E. Stanley, *Fractal Concepts in Surface Growth*, Cambridge University Press (1995).

[20] P.E. Kloeden and E. Platen, *Numerical Solution of Stochastic Differential Equations*, Springer, Berlin (1999).

[21] D.P.Landau and K. Binder, *A Guide to Monte Carlo Simulations in Statistical Physics*, Cambridge University Press (2005).

[22] C. Itzykson and J.-M. Drouffe, *Statistical Field Theory* v.2, Cambridge University Press (1989).